Innovative sensor networks for massive distributed thermal measurements in space applications under different environmental testing conditions

Original
Innovative sensor networks for massive distributed thermal measurements in space applications under different environmental testing conditions / Aimasso, A; Dalla Vedova, Mdl; Maggiore, P. - (2022), pp. 503-508. ((Intervento presentato al convegno 9th IEEE International Workshop on Metrology for AeroSpace, MetroAeroSpace 2022 tenutosi a Pisa (Italy) nel 27-29/06/2022 [10.1109/MetroAeroSpace54187.2022.9856275].

Publisher:
IEEE

Published
DOI:10.1109/MetroAeroSpace54187.2022.9856275

Innovative sensor networks for massive distributed thermal measurements in space applications under different environmental testing conditions

Alessandro Aimasso
Department of Mechanical and Aerospace Engineering
Politecnico di Torino
Turin, Italy
alessandro.aimasso@polito.it

Matteo D.L. Dalla Vedova
Department of Mechanical and Aerospace Engineering
Politecnico di Torino
Turin, Italy
matteo.dallavedova@polito.it

Paolo Maggiore
Department of Mechanical and Aerospace Engineering
Politecnico di Torino
Turin, Italy
paolo.maggiore@polito.it

***Abstract*— Optical fiber has seen significant development in the technical fields where it has been used in the last years. In the first place, obviously, for the Internet and, more broadly, to improve communication efficiency; but, more recently, for medicinal, structural, or lighting engineering applications. Furthermore, many optical solutions are beginning to be researched in the aerospace sector. The use of optical fiber, in particular, is strongly related to the employment of FBG type optical sensors, which may be particularly suitable for specific measurements of relevant physical parameters to be performed on specimens with typical aeronautical and/or space employment. More specifically, the performance of several FBG sensors for temperature measurement in vacuum for validation tests of space products has been examined during this work. Unlike typical thermocouples, the adoption of this new type of sensor can provide substantial benefits, beginning with a significant gain in terms of the size of the fiber, which ensures a minimum disturbance on thermal data. Furthermore, if supplied with a suitable coating (in polyimide), the optical fiber may guarantee a very high operating temperature range, which is extensively compatible with the high-temperature range existent in space. The measurements were divided into two independent phases. First, a preliminary test was performed in the laboratory using a climatic chamber to evaluate several sensor network integration methodologies on the specimens and select the most effective one for the vacuum test. The test demonstrated that a simple adhesive bonding of the fiber to the specimens ensures a precise temperature measurement under vacuum and stable conditions. The following vacuum test program confirmed that FBGs could be used as temperature sensors even at very high temperatures. The good results of this test encourage us to consider FBG strategic for space applications and, particularly, for thermal characterizations, thanks to the high number of available sensors, combined with the minimal cable's size. However, further studies are required in cryogenic cases to validate the entire range of extreme temperatures that characterize the space environment.**

Keywords*— *aerospace, distributed optical sensing, Fiber Bragg Gratings, FBG, onboard system, optical fibers, prognostics, sensors network, smart sensor, thermal measurements

I. INTRODUCTION

An optical fiber is a material made up of a glass cylindric structure that can carry light into itself. Because of this distinguishing feature, fiber's use has increased in recent decades, notably with applications in a wide range of industrial fields such as communications, medical diagnostics, lighting, the Internet, and many more. Optical fiber is now a key technology that is consistently employed in everyday applications, and it has a wide distribution throughout the global economy. The most well-known application of optical fiber nowadays is the construction of specific connections to enable increasingly efficient communications and faster Internet browsing speed. But thanks to some specific characteristics of this material, the use of the optical fiber has been resulted strategic also for the aerospace sector. Moreover, it could also be employed in sensor applications, thanks to the possibility of creating specific structures inside the fiber which act as a sensor, such as the case of Fiber Bragg Gratings (FBG) [1-7]. New types of sensors that combine high performance (in terms of sensitivity, accuracy, and reliability) with a high resistance to external disturbances (e.g., EM noise or electrostatic discharges) and other environmental conditions play a key part in current engineering projects and research [8-9]. All of these requirements are addressed by FBG sensors [10-11], which are appropriate for monitoring numerous technical characteristics in both static and dynamic modes. They might replace various standard sensors in aircraft [12-19], including structural monitoring, temperature management and compensation. They are also useful for space applications due to their resilience to electromagnetic interference, as well as their wide working temperature range and weight gain.

The study is carried out to quantify a relationship between the outputs generated by the FBG sensors and the environmental temperature for mechanically stable situations for space applications. The experimental test on the fiber was possible thanks to the collaboration with PhotoNext, the competence center on Photonics launched by POLITO in summer 2017.

A. Generalities about optical fiber and FBG

The optical fiber presents a cylindrical structure with several concentric layers: the *core*, the *cladding*, and the *coating*. The core is the most internal component, allowing the passage of the needed information in the form of a light signal.

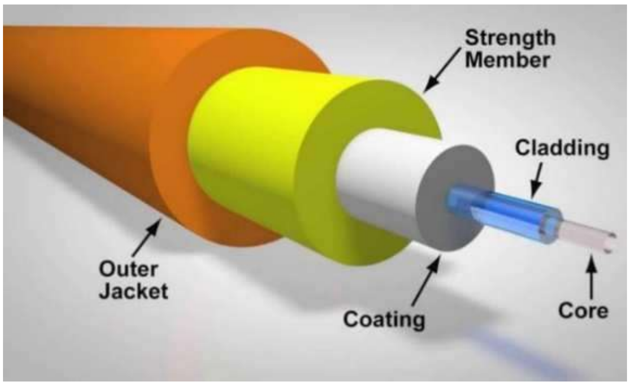

Fig. 1. The layers of an optical fiber

It is normally made of glass or a polymeric substance and has a maximum thickness of 50 µm. The cladding is the intermediate layer that is required to ensure the proper operation of the complete optical fiber. It has a diameter of 125 µm in general. The coating is the outer layer, and it is used to protect the structure from potential damage due to the fiber's extremely low bending resistance. Because of its high brittleness, several extra outer layers might be added to increase mechanical strength.

The physical principle at the base of the signal propagation into the fiber is the *Snell's law*:

$$n_1 sen(\theta_1) = n_2 sen(\theta_2) \tag{1}$$

where n_1 is the refraction index of material 1, n_2 is the refraction index of material 2, while Θ_1 is the incidence angle and Θ_2 the refraction angle. If the light beam is introduced in the core with an appropriate orientation, when it reaches the interface with the cladding, it will undergo a total reflection, so resulting confined within the optical fiber, allowing in this way the signal transmission. The maximum allowed angle for the light to enter in the fiber is calculated as:

$$\alpha_{\max} = arcsen\left(\frac{\sqrt{(n_1^2 - n_2^2)}}{n_0}\right) \tag{2}$$

where n_0 is the refractive index of the environment from the light comes. The sensors employed in the tests are Fiber Bragg Gratings (FBG). They are created in the fiber itself by employing a laser method to create a periodic fluctuation in the core refractive index. At the conclusion of this process, in a fiber trait of about 1 cm, there are some core bands with a new refractive index, resulting in $n_f = n_i + \Delta n$. Each of the parties with the changed refractive index is separated by a certain distance, denoted by the grating period Λ_G. This mechanism allows the sensor to function as a filter: when light passes through it, the FBG reflects a certain wavelength, known as the Bragg frequency, according to:

$$\lambda_B = 2 n_{EFF} \Lambda_G \tag{3}$$

where λ_B is the wavelength reflected by the FBG, n_{EFF} is the refractive index of the fiber (after the remodulation), Λ_G is the *pitch* of the grating as shown in Fig. 2. The Bragg frequency represents the output of the FBG sensor. The dependency of the Bragg frequency on the grating pitch, which is a physical distance, is shown in (3): this indicates that the fluctuation in the reflected wavelength is always related with a mechanical strain generated on the grating period by an external component.

As a result, it is simple to understand that loads applied to the sensor (in terms of induced strain) or thermal excursion create a significant variation in the reflected wavelength of the FBG, and so how wrote in (3) might be expressed as follows:

$$\Delta\lambda_B = K_\varepsilon \Delta\varepsilon + K_T \Delta T \tag{4}$$

In this way, the reflected wavelength is directly proportional to the strain and temperature variation applied to the sensor: the above-mentioned relation is then crucial in the process of sensor calibration conducted in the current study.

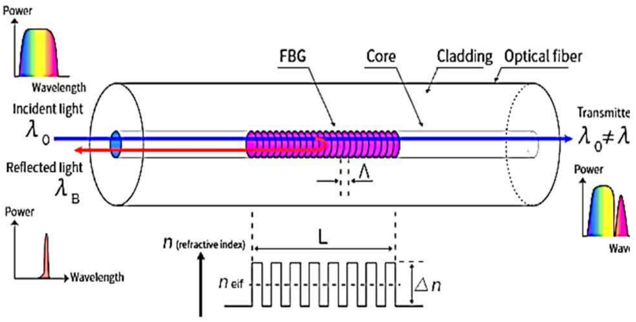

Fig. 2. Mechanism of working of an FBG.

B. FBG in space applications

The space environment is mainly characterized by its particularly hostile conditions, specifically in terms of temperature and high electromagnetic radiation. Consequently, the optical sensor technology in recent years has been particularly appreciated in space research projects above all for the following reasons:

- Low production costs;
- Low weight;
- Low cable's size;
- Immunity to electromagnetic disturbances;
- Possibility of having numerous embedded sensors in the same communication line;
- Possibility of measure different physical parameters with the same technology;
- High operative temperature ranges.

Thanks to the huge potential offered by optical fiber, FBGs have been integrated in several space systems, particularly for temperature measures, vibration analysis and test in vacuum for specific components thermal characterization. For example, recent FBG space applications covered propulsion tank's temperature control, thanks to the fiber's immunity to electromagnetic rays and its electrical passivity. Furthermore, the ESA mission Probe-2 employed these sensors directly for in-orbit thermal test, while other studies involved optical technology for temperature detection of specific space system [21-22].

Aim of this work, instead, is to evaluate FBG sensitivity to the thermal excursion in vacuum in mechanical stable configurations, in order to make the technology reliable for thermal characterization of space components during the test phases. The overall activity was so organized into two distinct parts: at first, a preliminary test in climatic chamber was conducted to select the better sensors integration strategy; and then the measures are repeated in vacuum.

II. THE EMPLOYED INSTRUMENTATION

As described at the end of the Introduction, to pursue the aim of this work two different measurement cycles are performed, each one with the specific optical instrumentation, already employed by the research group for other studies [20]. So, the overall data detection system includes optical fibers and FBG, a laser FBG interrogator, electronic temperature sensors (SHT85 and thermocouples), Arduino UNO, structural supports, a climatic chamber and a thermos-vacuum chamber.

A. *Optical fiber and FBG*

During the tests, at first two optical fibers with polyacrylate coating were used. One was pre-tensioned and glued to the metal support with an epoxide resin, while the other was simply adhered to the metal plates with a simple adhesive. Then, in the second part of the test campaign, four fibers with polyimide coating replaced the previous ones to operate at extended temperature ranges.

B. *FBG interrogator*

The FBG interrogator is the device that can automatically recognize and question the FBGs in the fibers connected to the various channels, as well as collect and analyse their responses. It communicates separately with each sensor, reducing the possibility of data misunderstandings from various FBG. The interrogator sends a laser beam through the fiber and measures the wavelengths reflected back. A SmartScan SBI laser interrogator created by the Smart Fibres society was employed in this application. The system runs a data acquisition loop once per minute, with each loop lasting one second and sampling at a variable frequency from 2.5 to 25 kHz. The average of all data acquired in a specific measurement on a given Bragg is obtained, generating the related instantaneous wavelength value.

C. *Electronic sensors*

Two kinds of electronic sensors were employed: in the first part, the climatic chamber was equipped with SHT85 sensors, while the thermo-vacuum chambers had got thermocouples.

SHT85 are electronic sensors that measure both the local temperature and humidity (thus providing an indication of the actual conditions to which the FBGs are subjected). This sensor operates at temperatures ranging from -40 to +105 °C and measures relative humidity levels spanning from 0% to 100%. These sensors are set to collect temperature and relative humidity measurements for the same time interval as the Smart Scan.

Instead, the *thermocouple* is a temperature transducer whose operation is based on the Seebeck effect.
Shortly, the thermocouple consists of two conductors of well-known material that are joined at a point called the "hot junction" near which the temperature measurement is to be made. The other two ends are connected to a terminal block called the "cold junction", which can be connected to the measuring instrument either directly or by means of an extension cable.

Fig.3. The employed FBG interrogator.

D. *Arduino Uno*

The Arduino Uno is the electronic board that will receive and communicate data from SHT85 sensors. It transmits sensor data to a personal computer (PC) via a USB connection. Python code is used to save these data. Finally, a MATLAB script is employed to perform an overall post-processing analysis.

E. *Climatic chamber*

The climatic chamber (model *kk50* made by 5Pascal) is able to control both temperature and relative humidity. Temperatures from -40 °C to 180 °C and relative humidity levels of 35% to 100 % are guaranteed. The machine assures a sensitivity of 0.1 °C and 1% humidity, and the temperature change speed can be adjusted from 1 to 300 °C/h. The humidity control of the chamber was not used for the measurements performed in this work.

F. *Thermo-vacuum chamber*

The thermos-vacuum chamber is strategic for testing space applications: in fact, by simultaneously controlling pressure and temperature in a well-defined volume of space, the space environmental conditions are recreated, where the only methods of heat transfer are conduction and radiation.

The chamber can depressurize the test environment down to values of 1*10-8 mbar, while working in temperature ranges between -190 °C and +160°C and the minimum temperature value is dictated by the use of nitrogen.

These temperature and pressure ranges can vary depending on the thermal and pumping capabilities of the vacuum chamber. The temperature ranges, for example, can be extended to both high and low temperatures using respectively heating lamps (IR or solar simulation) and/or cryocoolers based on the thermodynamics of helium that allows to theoretically reach the temperature of deep space.

III. TEST CAMPAIGNS

The test campaign conducted in this work is articulated into two distinct phases. At first, several measurement cycles were performed by employing a climatic chamber. During this test, the scope was to understand if pre-tensioning was necessary in order to obtain reliable temperature data in a mechanically stable situation. After this, the selected strategy is then employed in the thermo-vacuum chamber for the last part of our test campaign.

A. *Test conducted in climate chamber*

In the beginning, a preliminary test was conducted in a climate chamber to analyze the performance of FBG thermal sensors to verify their stability, accuracy, and sensitivity to operating conditions.

In particular, these former measures have been performed by comparing two different methods of their fixing, and then applying the best situation in the vacuum chamber. So, a first fiber was pretensioned and then glued on metal supports, while a second one was only adhered to them.

Thanks to the use of the climatic chamber, the sensors are exposed to a really significant thermal excursion. As already described, a first fiber was glued on two metal supports using the *Araldite* glue. During the gluing phase, using a micro mover, the fiber was also subjected to a constant tension which caused a deformation of about 1500 με. Once the transitory phase of the glue's viscous assessment is ended [20] the fiber was ready for the measurement. Instead, the second fiber was only adhered to the metal surface using a simple adhesive and then immediately ready to be tested. The above-mentioned set-up has got some temperature constraints:

- The glue cannot work over 90°C;
- The electronic sensors have an operative range of -40-125 °C;
- The acrylate coating of the fiber employed works well only up to about 120 °;
- The climatic chamber can guarantee thermal excursion from -40 to 180 °C.

For this reason, taking in consideration all the constraints, the overall detected temperature range covered the interval from -40 °C to +90 °, which anyway is a data range sufficiently extended for appropriate statistical considerations.

Some first measurement cycles were carried out in order to select the best data acquisition technique. In particular, it was crucial to regulate the velocity of the temperature change during the process to avoid possible delay between the fiber and the electronic responses in the calibration process. From this initial analysis, an excellent reactive ability of the FBG sensor was observed at slopes up to 20 °C per hour. At contrary, for thermal excursions velocities higher than 150 °C per hour, the fiber showed a gradually greater delay in its reaction the temperature change. Moreover, for the same high change rates, it resulted that the chamber did not reach a sufficient thermal equilibrium to make the measurements reliable. As a result, in order to minimize unwanted effects and errors, a speed of 20 degrees/hour was finally adopted for the measurements that will be shown below.

The analysis of the FBG performances covered several steps:

- To detect raw data
- To calculate the lambda/T curve
- To convert the FBG output into a T value
- To calculate the error.

At first, raw data are collected. Then the sensor characteristic is created using the experimental values obtained. This is the λ(T) relation and it explains the correlation between increasing temperature and sensor output, without considering the chronological time history of the setup temperature.

The λ(T) relation is explained in terms of:

$$\lambda(T) = \lambda_0 + K_T T \qquad (5)$$

where K_T and λ_0 are the angular coefficients and the known term of the linear fit calculated from the experimental data. Moreover, considering that sensors have got different nominal Bragg wavelength, the relation could be normalised as follow:

$$\frac{\Delta\lambda}{\lambda} = k_0 + k_T T \qquad (6)$$

From this calibration, it is possible to convert the FBG reflected wavelength into a temperature value using the equation:

$$T(\lambda) = \frac{\lambda - \lambda_0}{K_T} \qquad (7)$$

To generalize the relation, the temperature could be calculated from the normalised relation as follow:

$$T(\lambda) = \frac{\left(\frac{\Delta\lambda}{\lambda}\right) - k_0}{k_T} \qquad (8)$$

The initial thermal cycle performed in chamber covered the range between -40 °C and +40 °C. However, the relation λ(T) which resulted from the raw data highlighted how negative temperatures show a trend that differs in a not negligible way from the linear fit carried out. This means that when the wavelength values coming from FBG are converted into temperature – according to (7) – the resulting measures could have a significant error. In the subsequent measurement cycles, therefore, a temperature interval from 0 °C to +90 °C was considered: as shown in the figure, the results generally showed a much more stable trend. The instability of the λ(T) trend noticed in the colder interval and vice versa the better results obtained in the second temperature range were verified in both the fiber under analysis.

The results obtained in this first activity have therefore made possible to verify and quantify the linear correlation between the environmental temperature variation and the wavelength reflected by the FBG sensors, according to (5) and (6). Furthermore, the data showed a great influence of the bonding technique during the calibration process: indeed, despite the FBGS in the two fibers had the same nominal Bragg frequency, the coefficients K_T resulted different, as effect of the applied tension. The proportionality coefficients acquired from the linear fit (5) were utilized to translate FBGs outputs into temperature measures using (7), and finally the resulting trends were compared to how detected by typical electronic sensors.

As already said, the first measurement cycle, involving FBGs between -40 °C and +40 °C, highlighted a non-perfect linear trend during the calibration process. Therefore, converting the optical data by using (7), the temperature trend detected by the FBG was affected by a not negligible error. This does not mean that FBGs are not employable at low temperature, but only that more accurate calibration process is necessary and the linear fit here described gives not sufficient reliable data under 0 °C. At contrary, considering the temperature range from 0 °C to 90 °C, thanks to the stronger and more stable data linearity, after the calibration FBGs read the temperature variation with significantly higher reliability. So operating, the analysis showed really better results, enhancing the minimum difference between temperature detected by the fiber and how detected by the SHT85 sensor.

Finally, in order to select the better strategy for integrating sensors in the tested system in vacuum, two main aspects shall be kept in touch: the errors trends (calculated as the difference between the temperature measured by the free or pre-loaded

	Free	Tensioned
K_T	0.0107	0.0211
λ_0	1549.7	1547.0
RMSE	0.2679	0.4560

Table 1. Parameters of linear fits of the two fibers

fiber on and the electronic sensors) and the feasibility of the sensors implementation.

For what concerning the error, it is a bit lower in the free fiber. However, it is interesting underlying how, as observed in other our previous test campaigns, [23] this is true only in really mechanical stable situation. Indeed, when disturbances (such as high turbulent flow) covered the FBG, the tensioned fiber present a significantly larger wavelength excursion and, therefore, casual perturbations in the measurement (caused for example by small random mechanical phenomena and above all by the air convective flows) appear to be almost insignificant. More precisely, the amplitude of the disturbance on the signal is about the same, but in the tensioned fiber, this relates to an overall Δλ that is nearly an order of magnitude higher, rendering these oscillations practically inconsequential. From this, we can deduce a very high fiber sensibility to the environmental conditions, above all to mechanical solicitations. This is crucial, because if not effectively filtered, noise could cause very incorrect thermal calibrations: indeed, the strategy presented in this work is correct only in mechanical stable conditions.

In conclusion, the free fiber solution proved to be much easier to implement, and in presence of mechanical stable configurations, as it is the current set-up here analyzed, resulted a bit more precise the pre-loaded one too. For these reasons, the selected strategy is the free fiber simply adhered to a metal support, even if it shall be considered that an eventual undesired disturb in a more complex structure would generate a big error.

B. *Test conducted in vacuum*

Following the results of the laboratory tests in the climatic chamber, the FBG sensor network was transferred to the thermo-vacuum chamber, where measurements were taken across a wide temperature range of 0 °C to 200 °C. To withstand the high thermal excursion, optical fibers with a polyimide coating were used. The sensors were attached using a simple adhesive and without tensioning the fiber. The first thermal cycle was performed at temperatures ranging from -60 °C. to 150 °C. The same previous steps are followed for this test, and thus:

- To detect raw data
- To calculate the lambda/T curve
- To convert the FBG output into a T value
- To calculate the error.

The equations used to convert raw data into temperature values are the same already described in the previous paragraph. From the first temperature range evaluated (-100 °C/ +200 °C), as already seen during the measures in the climatic chamber, in the negative temperature the linearity was not well enhanced. For this reason, only positive temperature steps in this test were considered. The experiment covered different steps of about 15 minutes with stable temperature and then the transitory phase.

The final results are showed in Fig. 4 and Table 2. The T(λ) characteristic was discovered to highlight very well the linear relationship that correlates the temperature trend to the variation of the FBG output. In particular, about the coefficient K_T, it is really interesting to notice how the value is similar to that detected with the free fiber in the test conducted in climatic chamber. Thanks to this, the FBGs results applicable in vacuum in the same way as in the atmosphere, and then useful for both aeronautical and space applications.

Consequently, the errors detected after the sensors' outputs conversion in temperature data resulted low. Moreover, it appears that the creation of the vacuum prevents the presence of mechanical disturbance caused by the air's convective motion, which was previously detected in non-vacuum measurements, on all of the sensors examined. However, the bonding technique used in a vacuum was more important than in a climatic chamber. It is especially critical to select materials that are thermally stable and, above all, giving pay attention to do not fix materials with significant different thermal expansion coefficient and to put the adhesive correctly. In fact, during one cycle, a misplacement of the adhesive caused disturbances and mechanical stresses, rendering the measurements unreliable.

Anyway, the data stability of our measures demonstrates how optical fiber could be very useful, particularly in temperature characterization to test components for space applications. Because of its high sensitivity, it can detect even minor temperature variations, and its overall dimensions are much smaller than those of traditional sensors (thermocouples). Finally, unlike thermocouples, FBGs have got a shorter reaction time and thus detects sudden thermal changes immediately. Furthermore, having multiple Bragg sensors along the same optical fiber allows to have precise information in multiple points with a single cable, whereas

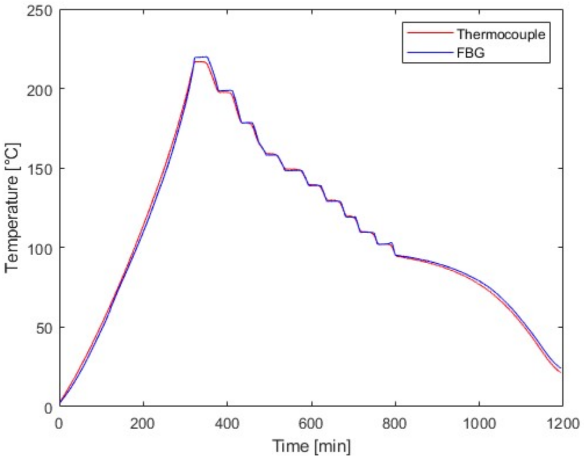

Fig. 4. Comparison between temperature values detected

Parameter	Value
K_T	0.0134
λ_0	1544.36
RMSE	1.1468

Table 2. Parameters of final test

electronic thermocouple sensors provide a one for each device, causing a bigger disturb.

The measurement campaign demonstrated how the FBG can be used safely up to 200 °C operating temperatures, a value that most traditional electronic sensors (other than thermocouples) very rarely support. Finally, but really important, it should be considered how all of these benefits were obtained solely by adhering the fiber to the plate, which is a very simple application method, certainly much simpler than pre-tensioning. Also, in this situation, we can infer that the low temperatures are not well interpolated by the linear fit resulting from the experimental data for the positive temperature. Indeed, we discovered a non-linear behaviour at low temperatures, but as in the previous case, this does not rule out the use of FBG at low temperatures, but rather necessitates a more complex calibration system capable of accounting for the non-linearities of the sensors. Indeed, above all in the vacuum proof, the non-linearities appeared as influenced by the temperature, the material employed and, above all, the installation methodology applied.

IV. CONCLUSIONS

The experiment produced extremely positive and encouraging results, above all considering it was the first test about the topic.

At first, the correlation between the output of the FBG sensors and the temperature was demonstrated and quantified, validating these sensors for temperature detection. Moreover, this study confirms the exceptional fiber's sensitivity to environmental conditions, theoretically not only about temperature, but also to mechanics conditions. From the first test it resulted that to test space components in stable situations and in vacuum, free fiber could be sufficient to make very accurate thermal measures. As a result, it was decided to conduct the measurement cycle in vacuum employing a free fiber only fixed to the specimens, at temperatures typical of the space. In this way it is possible to obtain an instrument that is much easier to integrate on the supports to be tested, such as metal plates and/or thermal protection coatings. If the test is performed in structural (static) stability conditions, this measurement cycle emphasized the very high stability of the outputs and the complete elimination of mechanical interference. Finally, the ability of the FBG and polyimide fiber to function perfectly even at extremely high temperatures was demonstrated, also maintaining the previously observed linear correlation.

The good results of this test encourage to consider FBG strategic for space applications and, particularly, for thermal characterizations: thanks to the high number of available sensors, combined with the extreme limited cable's size. Further studies are required in cryogenic cases to be able to carry out a validation on the entire range of extreme temperatures that characterize the space environment.

REFERENCES

[1] Mihailov S J 2012 Fiber Bragg grating sensors for harsh environments Sensors 12(2) 1898–1918

[2] Mihailov S J, Grobnic D, Hnatovsky C, Walker R B, Lu P, Coulas D and Ding, H 2017 Extreme Environment Sensing Using Femtosecond Laser-Inscribed Fiber Bragg Gratings MDPI Sensors 17(12) 2909

[3] Habel J, Boilard T, Frenière J S, Trépanier F and Bernier M 2017 Femtosecond FBG written through the coating for sensing applications MDPI Sensors 17(11), 2519

[4] Grobnic D, Mihailov S, Smelser C W and Ding H 2004 Sapphire Fiber Bragg Grating Sensor Made Using Femtosecond Laser Radiation for Ultrahigh Temperature Applications IEEE Photonics Technology Letters 16(11), 2505–2507

[5] Santos J L and Farahi F 2018 Handbook of Optical Sensors CRC Press

[6] Ahuja D and Parande D 2012 Optical sensors and their applications J. Sci. Res. Rev. 1(5), 60–8

[7] Giurgiuntiu V 2016 Structural health monitoring of aerospace composites Fiber-Optic Sensors

[8] Kersey A D 1996 A review of recent developments in fiber optic sensor technology *Optical Fiber Technology* 291–317

[9] Xin G, Zhengying L, Fan W, Yiming W, Changjia W, Siyue Z and Haihu Y 2017 *Optics Express* 25, 28112

[10] Berri P C, Dalla Vedova M D L, Maggiore P and Scolpito T 2019 Feasibility study of FBG-based sensors for prognostics in aerospace applications *Journal of Physics: Conference Series* 1249, 012015

[11] Dalla Vedova M D L, Berri P C, Maggiore P and Quattrocchi G 2020 Design and development of innovative fbg-based fiber optic sensors for aerospace applications *Journal of Physics: Conference Series* 1589, 012012

[12] Tanaka N, Okabe Y and Takeda N 2003 Temperature-compensated strain measurement using fiber Bragg gratings sensors embedded in composite laminates *Smart Materials and Structures* 12(6), 940–946

[13] Brusa E, Dalla Vedova M D L, Giorio L and Maggiore P 2021 Thermal condition monitoring of large smart bearing through fiber optic sensors *Mechanics of Advanced Materials and Structures* 28(11) 1187–1193

[14] Quattrocchi G, Berri P C, Dalla Vedova M D L and Maggiore P 2021 Optical fibers applied to aerospace systems prognostics: design and development of new FBG-based vibration sensors *IOP Conference Series: Materials Science and Engineering* 1024, 012095

[15] Dalla Vedova M D L, Quattrocchi G, Berri P C and Maggiore P 2021 Preliminary Analysis on Environmental and Intrinsic Factors on FBG-Based Vibration Sensors *Journal of Physics: Conference Series* 1977(1), 012011

[16] Liu L, Zhang H, Zhao Q, Liu Y and Li F 2007 *Optical fiber technology* 13, 78–80

[17] Kisala P and Cieszczyk S 2015 *Applied Optics* 54, 2677–2687

[18] Wenyuan W, Yongqin Y, Youfu G and Xuejin L 2015 Measurements of thermo-optic coefficient of standard single mode fiber in large temperature range *Proc. Int. Conf. Optical Instr. and Tech.: Optical Sensors and applications*, 9620

[19] Berri P C, Dalla Vedova M D L, Maggiore P and Secci C 2020 Fiber Bragg gratings for prognostics in space applications: a thermo-mechanical characterization of minimally invasive sensing techniques *Proc. 1st Aerospace Europe Conference AEC 2020* (Bordeaux)

[20] Berri P C, Dalla Vedova M D L, Aimasso A, (2021) Environmental sensitivity of Fiber Bragg Grating sensors for aerospace prognostics, *Proceedings of the 31st European Safety and Reliability Conference.*

[21] Iain McKenzie A, Ibrahim S, Haddad E, Abad S, Hurni A and Cheng L, (2021) Fiber Optic Sensing in Spacecraft Engineering: An Historical Perspective From the European Space Agency, *Frontiers in Physics.*

[22] Ibrahim S K, Farman M, O'Dowd J, Fiber sensing for space applications, 2018, Conference Paper

[23] Aimasso A, Dalla Vedova M D L, Maggiore P, Quattrocchi G, Study of FBG-based optical sensors for thermal measurements in aerospace applications, 2021, AIVELA Conference paper, in press.